

Enhancing quantum temporal steering via frequency modulation

Mengkai Wu(吴孟凯) and Weiwen Cheng(程维文)

Citation: Chin. Phys. B, 2024, 33 (**5**): 050306. DOI: 10.1088/1674-1056/ad2505
Journal homepage: http://cpb.iphy.ac.cn; http://iopscience.iop.org/cpb

What follows is a list of articles you may be interested in

Genuine entanglement under squeezed generalized amplitude damping channels with memory

Mazhar Ali

Chin. Phys. B, 2024, 33 (**2**): 020307. DOI: 10.1088/1674-1056/ace15f

Quantum interferometric power and non-Markovianity in the decoherence channels

Shaojie Xiong(熊少杰), Zhe Sun(孙哲), and Xiaoguang Wang(王晓光)

Chin. Phys. B, 2023, 32 (**8**): 080302. DOI: 10.1088/1674-1056/accb4e

Circuit quantum electrodynamics with a quadruple quantum dot

Ting Lin(林霆), Hai-Ou Li(李海欧), Gang Cao(曹刚), and Guo-Ping Guo(郭国平)

Chin. Phys. B, 2023, 32 (**7**): 070307. DOI: 10.1088/1674-1056/accd57

Generation of microwave photon perfect *W* states of three coupled superconducting resonators

Xin-Ke Li(李新克), Yuan Zhou(周原), Guang-Hui Wang(王光辉), Dong-Yan Lv(吕东燕),Fazal Badshah, and Hai-Ming Huang(黄海铭)

Chin. Phys. B, 2023, 32 (**4**): 040306. DOI: 10.1088/1674-1056/aca394

Enhancement of electron-positron pairs in combined potential wells with linear chirp frequency

Li Wang(王莉), Lie-Juan Li(李烈娟), Melike Mohamedsedik(麦丽开·麦提斯迪克), Rong An(安荣), Jing-Jing Li(李静静), Bo-Song Xie(谢柏松), and Feng-Shou Zhang(张丰收)

Chin. Phys. B, 2023, 32 (**1**): 010301. DOI: 10.1088/1674-1056/ac744b

---

Enhancing quantum temporal steering via frequency modulation

Mengkai Wu(吴孟凯) and Weiwen Cheng(程维文)†

Institute of Signal Processing & Transmission, Nanjing University of Posts and Telecommunication, Nanjing 210003, *China*

(Received 3 December 2023; revised manuscript received 20 January 2024; accepted manuscript online 2 February 2024)

Various strategies have been proposed to harness and protect space-like quantum correlations in different models under decoherence. However, little attention has been given to temporal-like correlations, such as quantum temporal steering (TS), in this context. In this work, we investigate TS in a frequency-modulated two-level system coupled to a zero-temperature reservoir in both the weak and strong coupling regimes. We analyze the impact of various frequency-modulated parameters on the behavior of TS and non-Markovian. The results demonstrate that appropriate frequency-modulated parameters can enhance the TS of the two-level system, regardless of whether the system is experiencing Markovian or non-Markovian dynamics. Furthermore, a suitable ratio between modulation strength and frequency (*i.e.*, all zeroes of the 0th Bessel function $J_0(\delta/\Omega)$) can significantly enhance TS in the strong coupling regime. These findings indicate that efficient and effective manipulation of quantum TS can be achieved through a frequency-modulated approach.

Keywords: quantum temporal steering, frequency modulation, decoherence

PACS: 03.65.Ud, 03.65.Yz, 03.67.Mn **DOI:** 10.1088/1674-1056/ad2505

1. Introduction

Quantum steering is an intriguing phenomenon that allows one party to manipulate a quantum state on another party remotely through local operations. This concept, which challenges our common sense, has attracted significant attention in various fields of physics in recent years, both in theoretical analysis and experimental exploration.[1–17] Researchers have devised steering inequalities to detect this nonlocal correlation that provides evidence of quantum steering when violated.[18–20] Moreover, quantum steering is highly promising in quantum information processing. It has been successfully applied in developing one-sided device-independent quantum key distribution,[13] secure quantum teleportation,[14] and one-way quantum computing.[16] While spatial quantum steering has garnered significant attention and sparked extensive discussions, its temporal counterpart, quantum TS, has also generated notable interest.[21–27] In this scenario, Alice sends a quantum system to a remote recipient, such as Bob, via a designated quantum channel referred to as Λ. Nevertheless, before Bob receives and measures the quantum system, Alice can manipulate her quantum system using specific operations. This poses an intriguing question: What impact do Alice's operations have on the state of the system observed by Bob? Chen *et al*. introduced the concept of quantum TS and developed the TS inequality to address this question.[21,22] Similar to quantifying spatial quantum steering, measures such as TS weight[23] and robustness[24] have been proposed to evaluate this phenomenon. Moreover, quantum TS exhibits promising applications in quantum information processing, including quantum key distribution[21,23] and quantum non-Markovianity.[22]

On the other hand, open quantum systems undergo decoherence due to their interaction with the surrounding environment, which often leads to the destruction of quantum correlations. This limitation hinders their practical use in quantum information and metrology. Consequently, various strategies have been developed to control and preserve quantum resources,[28–34] including techniques like dynamical decoupling,[28] feedback control,[30] and the quantum Zeno effect.[33] Recent studies have unveiled the immense potential of modulating the transition frequency of a qubit as a fundamental tool to unveil a myriad of captivating phenomena.[35–45] These phenomena consist of the emergence of sideband transitions,[37,38] modification of the fluorescence spectrum,[39,40] and the enhancement of the degree of non-Markovianity.[41] Empirical investigations have successfully demonstrated the feasibility of frequency modulation in superconducting qubits.[35,43] Moreover, numerous studies have demonstrated that the frequency-modulation approach profoundly impacts the dynamics of space-like quantum correlations.[46–49] According to the definition of TS, the interaction between the quantum system and the environment inevitably affects the quantum state received by Bob. In simpler words, the noise from the environment considerably influences the temporal-like correlation between the system's states at different times. This leads us to question how to improve or safeguard these temporal-like quantum correlations in a noisy environment. In this work, we focus on examining the influence of frequency modulation on quantum TS. We aim to understand the underlying dynamics better by exploring how TS can be manipulated by incorporating frequency modulation.

In this study, we investigate the impact of frequency mod-

†Corresponding author. E-mail: wwcheng@njupt.edu.cn

© 2024 Chinese Physical Society and IOP Publishing Ltd

ulation on temporal-like quantum correlation. Our results reveal an interesting aspect: the appropriate parameters of frequency modulation can enhance the TS of the two-level system, regardless of whether the system is undergoing Markovian or non-Markovian dynamics. Moreover, a suitable ratio between the modulation strength and frequency, which corresponds to the zeroes of the Bessel function of order zero ($J_0(\delta/\Omega)$), can significantly boost TS in the strong coupling regime. Through an analysis of non-Markovianity, we demonstrate that the long-term preservation of TS is directly linked to the memory effect in the strong coupling regime. These findings suggest that effective and efficient manipulation of quantum TS can be achieved through the use of frequency modulation.

The remainder of this work is organized as follows. In Sections 2 and 3, we give a brief of introduce the model and the concept of quantum TS, respectively. In Section 4, we study and discuss the effect of frequency modulation parameters on TS both for weak coupling regime and strong ones. Finally, we give a summary of our results.

2. Model and solution

Here, we consider a qubit coupled to a zero-temperature reservoir formed by the quantized modes of a high-Q cavity. The transition frequency of the qubit is modulated sinusoidally by an external driving field. The Hamiltonian of the system is as follows:[46–50]

$$H(t)=\frac{1}{2}[\omega_0+\delta\cos(\Omega t)]\hat{\sigma}_z+\sum_k\omega_k\hat{\eta}_k^\dagger\hat{\eta}_k+\sum_k\{g_k\hat{\sigma}_+\hat{\eta}_k+g_k^*\hat{\sigma}_-\hat{\eta}_k^\dagger\}. \tag{1}$$

Here, $\hat{\sigma}_z$ is the Pauli matrix, $\hat{\sigma}_\pm$ represent the raising and lowering operators, $\hat{\eta}_k^\dagger$ and $\hat{\eta}_k$ are the creation and annihilation operators for a photon of mode k with the frequency ω_k. ω_0 denotes the transition frequency, δ and Ω are the modulation amplitude and frequency, respectively. By performing the following transformation:[36,46]

$$\hat{U}=\exp\left\{-\mathrm{i}\left[\sum_k\omega_k\hat{\eta}_k^\dagger\hat{\eta}_k t+\left[\omega_0 t+\frac{\delta}{\Omega}\sin(\Omega t)\right]\frac{\hat{\sigma}_z}{2}\right]\right\}, \tag{2}$$

the Hamiltonian can be transformed as

$$\widetilde{H}=\hat{U}^\dagger H\hat{U}+\mathrm{i}\left(\frac{\partial\hat{U}^\dagger}{\partial t}\right)\hat{U}=\sum_k g_k\hat{\sigma}_+\hat{\eta}_k\,\mathrm{e}^{-\mathrm{i}(\omega_k-\omega_0)t}\,\mathrm{e}^{\mathrm{i}(\delta/\Omega)\sin(\Omega t)}+\sum_k g_k^*\hat{\eta}_k^\dagger\hat{\sigma}_-\,\mathrm{e}^{\mathrm{i}(\omega_k-\omega_0)t}\,\mathrm{e}^{-\mathrm{i}(\delta/\Omega)\sin(\Omega t)}. \tag{3}$$

According to the Jacobi–Anger expansion, one can decompose the modulation terms into Fourier series as

$$\mathrm{e}^{\pm\mathrm{i}(\delta/\Omega)\sin\Omega t}=\mathrm{J}_0\left(\frac{\delta}{\Omega}\right)+2\sum_{n=1}^{\infty}(\pm\mathrm{i})^n\mathrm{J}_n\left(\frac{\delta}{\Omega}\right)\cos(n\Omega t), \tag{4}$$

where $\mathrm{J}_n(\delta/\Omega)$ denotes the n-th order Bessel function. We assume the initial states of whole system as

$$|\Phi(0)\rangle=\frac{1}{\sqrt{2}}(|e\rangle+|g\rangle)|0\rangle,$$

($|0\rangle$ denotes the vacuum state of the cavity), then the evolution state can be obtained as

$$|\Phi(t)\rangle=\frac{1}{\sqrt{2}}(\zeta(t)|e\rangle|0\rangle+|g\rangle|0\rangle)+\sum_k\zeta_k(t)|g\rangle|1_k\rangle, \tag{5}$$

for time t. Here, $|1_k\rangle$ denotes a single photon in mode k of the reservoir and $\zeta_k(t)$ represents its probability amplitude. By Solving the time-dependent Schrödinger equation, one obtains the integro-differential equation for $\zeta(t)$ as[49]

$$\dot{\zeta}(t)+\int_0^t\mathrm{d}\tau K(t,\tau)\zeta(\tau)=0, \tag{6}$$

where the kernel $K(t,\tau)$ is

$$K(t,\tau)=\exp\left[\mathrm{i}\left(\frac{\delta}{\Omega}\right)\{\sin(\Omega t)-\sin(\Omega\tau)\}\right]\times\int_0^\infty J(\omega)\,\mathrm{e}^{-\mathrm{i}(\omega-\omega_0)(t-\tau)}\,\mathrm{d}\omega. \tag{7}$$

Here, $J(\omega)$ indicates the spectral density of the reservoir modes, and adopts Lorentzian spectral distribution as[51]

$$J(\omega)=\frac{1}{2\pi}\frac{\gamma\lambda^2}{(\omega_0-\omega)^2+\lambda^2}. \tag{8}$$

Consequently, the kernel $K(t,\tau)$ can be obtained as follows:

$$K(t,\tau)=\frac{\gamma\lambda}{2}\,\mathrm{e}^{-\lambda(t-\tau)}\,\mathrm{e}^{\mathrm{i}(\delta/\Omega)[\sin(\Omega t)-\sin(\Omega\tau)]}. \tag{9}$$

By substituting it into Eq. (6), one gets

$$\dot{\zeta}(t)+\frac{\gamma\lambda}{2}\,\mathrm{e}^{\mathrm{i}(\delta/\Omega)\sin(\Omega t)}\int_0^t\mathrm{d}\tau\,\mathrm{e}^{-\mathrm{i}(\delta/\Omega)\sin(\Omega\tau)}\,\mathrm{e}^{-\lambda(t-\tau)}\zeta(\tau)=0. \tag{10}$$

Now, we can numerically solve the above equation to determine the probability amplitude $\zeta(t)$. And the reduced density matrix of the qubit can be expressed as[51]

$$\rho_s(t)=\begin{pmatrix}\rho_{11}(0)|\zeta(t)|^2 & \rho_{10}(0)\zeta(t)\\ \rho_{01}(0)\zeta^*(t) & \rho_{00}(0)+\rho_{11}(0)(1-|\zeta(t)|^2)\end{pmatrix} \tag{11}$$

in the standard basis $\{|e\rangle,|g\rangle\}$.

3. TS and its measurement

Here, we provide a brief introduction to the concept of quantum TS and its measurement. In the standard (*i.e.*, spatial) scenario of quantum steering, Alice performs a positive-operator valued measure measurement denoted by $M_{a|x}$ on her subsystem, while Bob shares the quantum state $\rho_{\rm AB}$. The measurement operator $M_{a|x}$ satisfies the conditions $\sum_a M_{a|x}=I$ and $M_{a|x}\geq 0$ for all possible outcomes (a) and measurement bases (x). Consequently, Bob is left with a non-normalized state assemblage denoted by $\{\sigma_{a|x}\}$, where $\sigma_{a|x}={\rm tr_A}[(M_{a|x}\otimes I)\rho_{\rm AB}]$. This process is schematized in Fig. 1(a). By employing the semi-definite program, one can verify whether the assemblage $\{\sigma_{a|x}\}$ belongs to the set of unsteerable or steerable ones.[3,4] In TS ones, Alice also performs a positive-operator valued measurement $M_{a|x}$ for an initial state ρ_0 at time $t=0$. Then the initial state is mapped to $\sigma_{a|x}(0)$,

$$\sigma_{a|x}(0)=\frac{M_{a|x}\rho_0}{p(a|x)} \tag{12}$$

with

$$p(a|x)={\rm tr}(M_{a|x}\rho_0).$$

Then the postmeasurement state $\sigma_{a|x}(0)$ is sent into a quantum channel Λ. At time t, Bob receives the assemblage $\sigma_{a|x}(t)=\Lambda[\sigma_{a|x}(0)]$, schematizing in Fig. 1(b).[22] Now, by checking the assemblage $\sigma^{\rm T}_{a|x}(t)\equiv p(a|x)\sigma_{a|x}(t)$ whether it can be written in the following local hidden-state form:[22,24]

$$\sigma^{\rm T}_{a|x}(t)=\sigma^{\rm T,US}_{a|x}=\sum_\lambda P(\lambda)P(a|x,\lambda)\sigma_\lambda. \tag{13}$$

If the above expression is true, Bob refers to such an assemblage as unsteerable. This means that the states he received were not actually influenced by Alice's measurement. On the other hand, if the expression is false, Bob refers to such an assemblage as steerable, which implies that the state he received was actually influenced by Alice's measurement. Similar to the concept of quantum space-like steering robustness, the scenario can be extended to quantum TS robustness $R(\{\sigma^{\rm T}_{a|x}(t)\})$. By determining the amount of noise that needs to be added to a given temporal assemblage $\{\sigma^{\rm T}_{a|x}(t)\}$ in order for it to satisfy a local hidden state model, the quantum TS robustness of a temporal assemblage $\{\sigma^{\rm T}_{a|x}(t)\}$ can be defined as follows:[4,5]

$$\begin{aligned}R(\sigma^{\rm T}_{a|x}(t)) &= \min_{\sigma^{\rm T}_{a|x},\sigma_\lambda,t}\ \nu\ \ {\rm s.t.}\frac{\sigma^{\rm T}_{a|x}(t)+\nu\tau_{a|x}}{1+\nu}\\ &=\sum_\lambda D(a|x,\lambda)\sigma_\lambda\ \ \forall a,x\\ &\tau_{a|x}\in\mathcal{N},\quad \sigma_\lambda\geq 0\ \forall\lambda.\end{aligned} \tag{14}$$

Here, $\mathcal{N}$ is any subset of assemblages characterised by positive semi-definite constraints and linear matrix inequalities. Then, we can take the temporal steering robustness $R_{\rm TS}$ as a measure of steerability of the temporal assemblage $\{\sigma^{\rm T}_{a|x}(t)\}$.

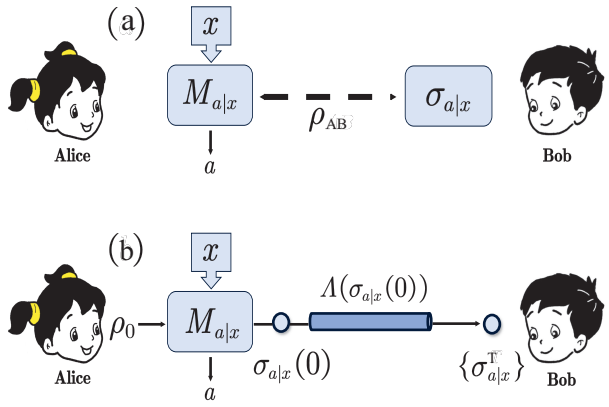


Fig. 1. (a) Sketch of quantum steering from Alice to Bob, in which $\rho_{\rm AB}$ represents the shared state. (b) Sketch of quantum TS. Firstly, Alice take a measurement $M_{a|x}$ on the initial state ρ_0. Then, ρ_0 is mapped to $\sigma_{a|x}(0)$ and sent into a quantum channel Λ. Finally, Bob receives the assemblage $\{\sigma^{\rm T}_{a|x}\}$ at time t.

4. Results and discussion

We begin the quantitative analysis by examining the time evolution of TS under a weak coupling regime ($\lambda=3\gamma$), as shown in Fig. 2. We consider various values of the modulation frequency Ω while keeping a constant modulation amplitude of $\delta=10\gamma$. Additionally, we compare this evolution to the case where the external driving is turned off ($\delta=0$), which leads to the disappearance of TS at time t_0. As observed, the behavior of TS depends on the parameter Ω under the given condition for δ. For smaller values of Ω (e.g., $\Omega=0.001\gamma$ or 0.1γ), TS persists for longer durations than t_0. However, frequency modulation does not positively impact the TS for a larger modulation frequency, such as $\Omega\geq 100\gamma$. As in these cases, TS does not survive longer than those without frequency modulation. For instance, the orange-dash line (corresponding to the case $\Omega=100\gamma$) overlaps with the black-solid one. Notably, TS exhibits oscillatory behavior in its dynamics for specific modulation frequencies (e.g., $\Omega=1.0\gamma$ or 5.0γ), indicating the presence of non-Markovian effects even under a weak coupling regime.[50]

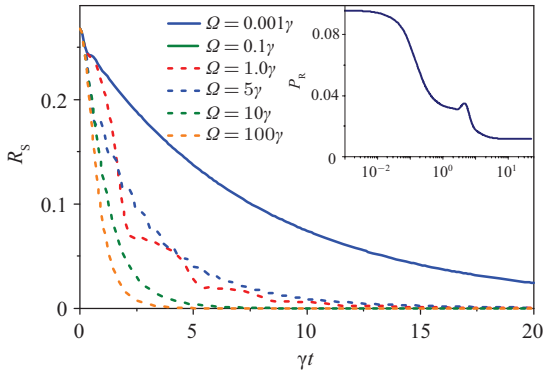


Fig. 2. Main: temporal steering robust R_S as a function of scaled time γt for different values of the modulation frequency Ω. The values of other parameters are: $\delta = 10\gamma$, $\lambda = 3\gamma$ (weak coupling). Insert: temporal steering robust power P_R as a function of modulation frequency Ω. Hereafter, solid black line corresponds to the situation in which frequency modulation is off, i.e., $\delta = 0.0$.

To highlight the effect of the frequency modulation parameter Ω on TS, we take a strategy to calculate the TS power P_R as follows:

$$P_R := \frac{1}{T_b}\int_0^{T_b} R_S(t)\,dt. \tag{15}$$

Here, P_R represents the average value of R_S throughout evolution T_b. Consequently, it effectively considers the effects of time evolution on R_S. This means that the characterization of frequency modulation will have a more prominent role in the TS. In the insert of Fig. 2, we have included a plot showing the relationship between P_R and the modulation frequency parameter Ω. The results generally show that the robustness power of TS, P_R, becomes more significant as Ω decreases, especially in the weak coupling regime. This indicates that frequency modulation can enhance the TS of the two-level system, both in the Markovian and non-Markovian regions. Interestingly, we observe a local maximum for P_R at around $\Omega \simeq 4.16\gamma$, which corresponds to the first zero of the Bessel function $J_0(\delta/\Omega)$.

As shown above, the behavior of TS is dependent on the modulation frequency Ω for a fixed modulation strength δ. Figures 3(a)–3(c) illustrate a family of TS concerning γt under different values of δ while considering varying modulation frequencies Ω such as 0.1γ, 1.0γ, and 5.0γ. The common feature observed in Figs. 3(a)–3(c) is that TS becomes more significant as the modulation strength δ increases, while the modulation frequency Ω remains fixed. However, the impact of modulation strength on TS varies depending on Ω. For example, in Fig. 3(a), where $\Omega = 0.1\gamma$, TS only marginally increases with an increasing δ, and the dynamics of TS exhibit a monotonous behavior. On the other hand, in Fig. 3(c), where $\Omega = 5\gamma$, TS experiences a significant increase with a more considerable modulation strength δ, and the TS dynamics are accompanied by rapid and minor oscillations. In the case of $\Omega = 1.0\gamma$, as shown in Fig. 3(b), TS increases with a larger δ and is accompanied by significant oscillations.

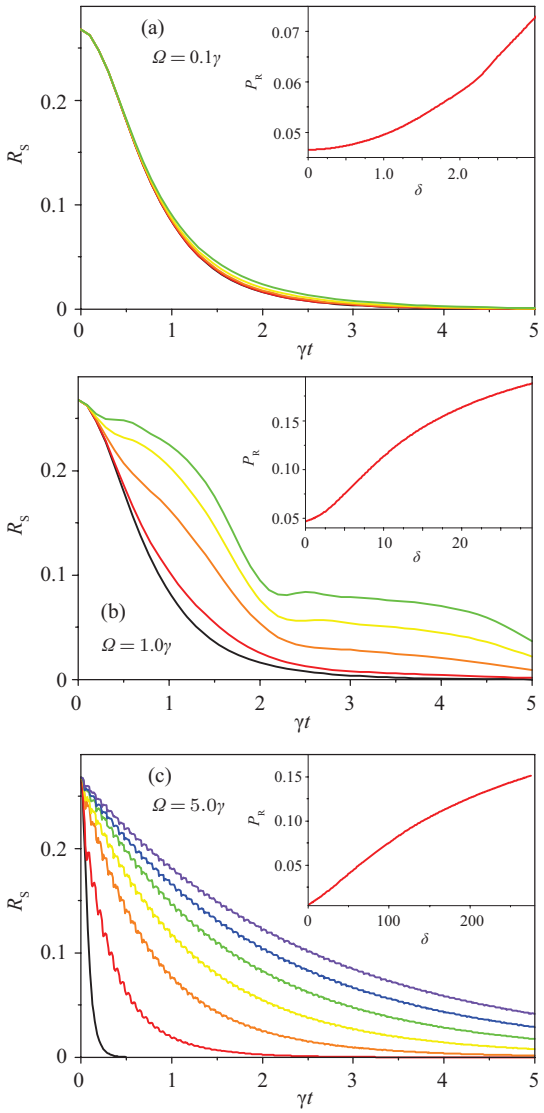


Fig. 3. Main: temporal steering robust R_S as a function of scaled time γt for different values of the modulation strength: $\delta = 2.4048\Omega$ (red line), $\delta = 5.5201\Omega$ (orange line), $\delta = 8.6537\Omega$ (yellow line), $\delta = 11.7915\Omega$ (green line), $\delta = 14.9309\Omega$ (blue line), and $\delta = 18.0711\Omega$ (violet line). Insert: temporal steering robust power P_R as a function of modulation strength δ. In panels (a), (b), and (c), the modulation frequency Ω are taken 0.1γ, 1.0γ, and 5.0γ respectively. Here, $\lambda = 3\gamma$.

To explain the above behavior of TS qualitatively, two quantities (i.e., frequency shift $s(t)$ and decoherence rate $\xi(t)$) are calculated as

$$s(t) = -\mathrm{Im}\left[\frac{\dot{\zeta}}{\zeta}\right], \quad \xi(t) = -\mathrm{Re}\left[\frac{\dot{\zeta}}{\zeta}\right]. \tag{16}$$

When the frequency modulation is absent (e.g., $\delta = 0$, the black solid line shown in Fig. 4(a)), there is no frequency shift; however, the frequency shift would emerge with the presence of frequency modulation (e.g., $\delta \neq 0$), the red cross, yellow circle, and olive star shown in Fig. 4(a). A positive $\xi(t)$ value, e.g., the black solid line and the olive star shown in Fig. 4(a), implies a unidirectional flow of information from the system to

the environment, which means that the process is Markovian. On the other hand, negative $\xi(t)$ values suggest the emergence of information backaction from the environment, e.g., the red cross, yellow circle shown in Fig. 4(a). At this stage, we can also quantitatively calculate the non-Markovianity to determine whether the TS protection is connected to memory effects. To do so, we adopt the measure proposed by Breuer *et al.*, which can be expressed as[52]

$$N \equiv \max_{\rho_{1,2}(0)} \int_{\sigma>0} \mathrm{d}t\sigma[t, \rho_{1,2}(0)]. \tag{17}$$

The maximization run over all the possible pairs of initial density matrices. Furthermore, one can obtain the non-Markovianility as[53]

$$N = \frac{1}{2}\left[\int_0^{T_b} |\partial_\tau \xi(\tau)|\mathrm{d}\tau + |\xi(T_b)| - 1\right]. \tag{18}$$

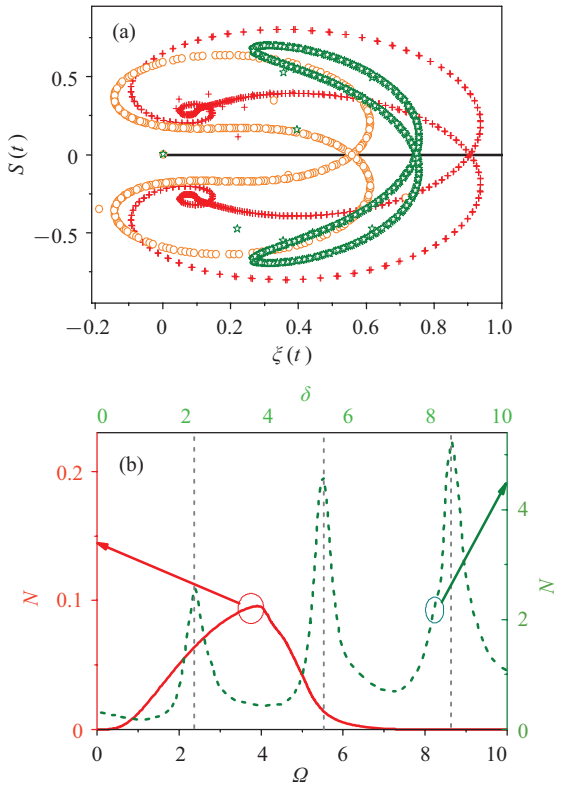


Fig. 4. (a) In the weak coupling regime ($\lambda = 3\gamma$), time evolution of frequency shift $s(t)$ and decoherence rate $\xi(t)$ for different values of modulation frequency: $\Omega = 1.0\gamma$ (red cross), $\Omega = 4.0\gamma$ (yellow circle), and $\Omega = 8.0\gamma$ (olive star). Here, $\delta = 10\gamma$. (b) Non-Markovian N as a function of Ω, with a red solid line representing the weak coupling regime (labeled on the left Y axis), and δ in the strong coupling regime shown as an olive dash line (labeled on the right Y axis, with parameters $\Omega = 1.0\gamma$, $\lambda = 0.1\gamma$.

In the weak coupling regime ($\lambda = 3\gamma$), we plot the degree of non-Markovianity (N) as a function of modulation frequency (Ω) with a fixed modulation amplitude of $\delta = 10\gamma$, as shown in Fig. 4(b). The plot reveals that there is no memory effect for minor modulation frequencies (e.g., $\Omega < 0.5\gamma$) or larger ones (e.g., $\Omega > 7.0\gamma$). However, frequency modulation can induce weak non-Markovian features in the weak-coupling regime for intermediate values of Ω (e.g., $\Omega = 1.0\gamma$ or 5.0γ).[50] This justifies the presence of oscillations in the time evolution of the TS for $\Omega = 1.0\gamma$ and $\Omega = 5.0\gamma$ (refer to Fig. 2). Furthermore, these findings are consistent with those shown in Fig. 4(a). Overall, these results suggest no direct relationship between non-Markovian and the promotion of TS in the weak coupling regime.

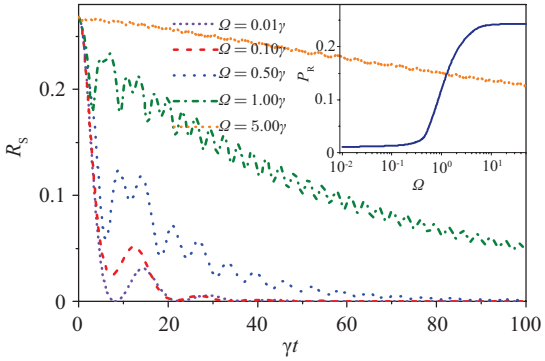


Fig. 5. (a) Temporal steering robust R_S as a function of scaled time γt for different values of the modulation frequency Ω. The values of other parameters are: $\delta = 2.4048\Omega$, $\lambda = 0.1\gamma$. (b) Temporal steering robustness power P_R as a function of modulation frequency Ω.

Another topic for analysis is the dynamics of TS in the strong coupling regime, precisely when $\lambda = 0.1\gamma$. In this regime, R_S behavior becomes more complex than the weak coupling regime. Figure 5 illustrates the evolution of R_S as a function of γt under various modulation frequencies Ω, with modulation strength $\delta = 2.4048\Omega$. This value corresponds to the first zero of the zeroth Bessel function $J_0(\delta/\Omega)$. For minor modulation frequencies such as $\Omega = 0.01\gamma$, $\Omega = 0.1\gamma$, and $\Omega = 0.5\gamma$, an increasing Ω leads to significant TS with noticeable oscillations. Interestingly, the shot-dash purple line, corresponding to $\Omega = 0.01\gamma$, almost overlaps with the black-solid line. However, as the modulation frequency increases, the oscillatory behavior of R_S decreases. This can be observed in the olive-dash-dot line ($\Omega = 1.0\gamma$) and the yellow-dash-dot-dot line ($\Omega = 5.0\gamma$) in Fig. 5. Moreover, TS persists for a longer duration when the modulation frequency is more significant, compared to the case of a minor modulation frequency Ω. Furthermore, R_S decays slower as the modulation frequency Ω increases. The insert in Fig. 5 shows the P_R plot as a function of the modulation frequency Ω. The results indicate that the temporal steering robustness power P_R becomes more significant with increasing Ω. In other words, the modulation frequency can enhance TS in the two-level system under the strong coupling regime. To gain a more comprehensive understanding of the effective TS protection, we have depicted the time-dependent decay rate $\xi(t)$ for various values of Ω in Fig. 6. The plots reveal that the decay rate can assume negative values during certain time intervals, indicating the coherent backaction from the environment and non-Markovian

characteristics. Despite the increasing frequency, the oscillation amplitude of the decay rate decreases significantly for a high modulation frequency Ω. These findings suggest that the prolonged preservation of TS mainly stems from the suppression of the decay rate $\xi(t)$ of the qubit.

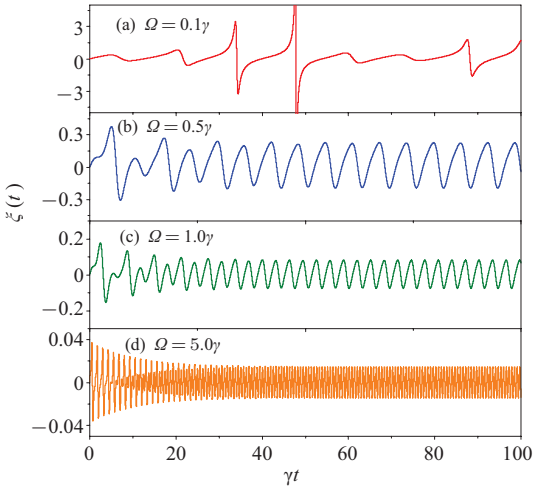


Fig. 6. Decoherence rate $\xi(t)$ as a function of scaled time γt for different values of the modulation frequency: (a) $\Omega = 0.1\gamma$, (b) $\Omega = 0.5\gamma$, (c) $\Omega = 1.0\gamma$, and (d) $\Omega = 5.0\gamma$. Other parameters are those of Fig. 5, that is, $\delta = 2.4048\Omega$, and $\lambda = 0.1\gamma$.

Figure 7 illustrates the dynamics of TS as a function of the scaled time γt in the strong coupling regime ($\lambda = 0.1\gamma$) with different modulation amplitudes δ for several values of the modulation frequency: (a) $\Omega = 0.1\gamma$, (b) $\Omega = 1.0\gamma$, and (c) $\Omega = 5.0\gamma$. A common feature in Figs. 7(a)–7(c) is that TS becomes more significant as the modulation strength δ increases, while the modulation frequency Ω remains fixed. However, the impact of modulation strength on TS varies significantly depending on Ω. For example, in Fig. 7(a), where $\Omega = 0.1\gamma$, TS sustained increases with an increasing δ, accompanied by intense oscillations. This is supported by the curve for $P_{\rm R}$ concerning δ in the insert. On the other hand, in Fig. 7(c), where $\Omega = 5\gamma$, TS experiences a significant increase when the ratio of amplitude and frequency of modulation (δ/Ω) is intentionally tuned to all zeroes of the 0-th Bessel function $J_0(\delta/\Omega)$ (e.g., $\delta = 2.4048\Omega$ (blue dot-dash line), 5.5201Ω (orange dash line), and 8.6537Ω (red dot line)) when compared with the case where δ/Ω does not meet those non-trivial points (e.g., those solid lines). The curve of $P_{\rm R} \sim \delta$ in the insert highlights this result. It is worth mentioning that Mortezapour et al. have argued that the optimal coherence preservation, controlled by qubit frequency modulation, occurs only when the conditions $\delta = 2.4048\Omega$ and $\Omega = 5.0\gamma$ are met.[46] However, our results suggest that the TS can be significantly maintained for all zeroes of the 0-th Bessel function $J_0(\delta/\Omega)$ under such circumstances. As a comparison, we also demonstrate the TS as a γt function with different δ for $\Omega = 1.0\gamma$, as shown in Fig. 7(b). Remarkably, it can be easily observed that an appropriate frequency modulation ratio of δ/Ω can also safeguard the TS from decoherence, particularly for the higher-order zeroes of the 0-th Bessel function $J_0(\delta/\Omega)$. Additionally, we find that the high TS protection found above is ultimately linked to strong memory effects by comparing with the degree of non-Markovianity (shown in Fig. 4(b)) and the TS power (shown in Figs. 7(b) and 7(c)).

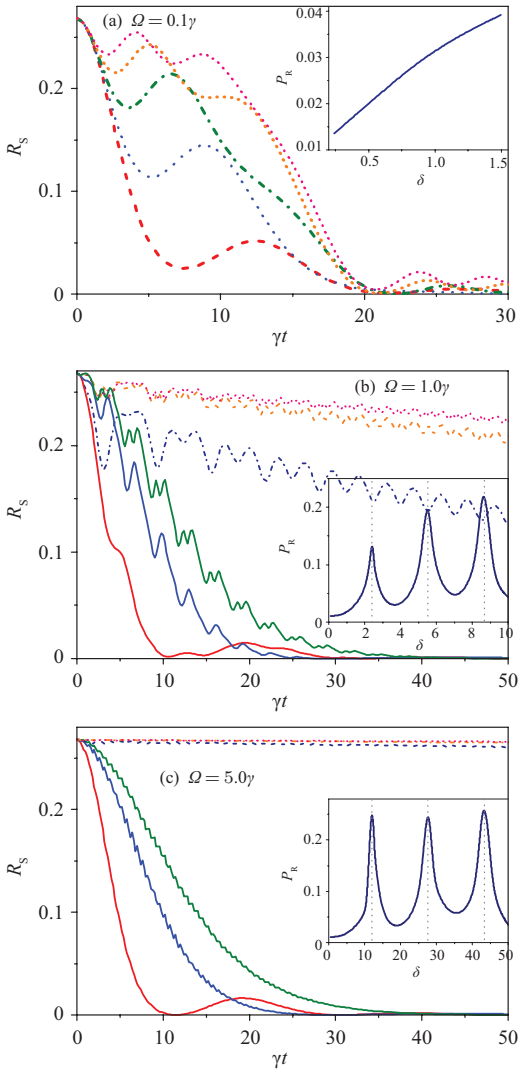


Fig. 7. Main: temporal steering robust $R_{\rm S}$ as a function of scaled time γt for different values of the modulation strength. Insert: temporal steering robust power $P_{\rm R}$ as a function of modulation strength δ. In panel (a), the modulation strength δ take the 1-st–6-th zeros of the $J_0(\delta/\Omega)$. In panels (b) and (c), the sold line for red, blue, and olive corresponding to modulation strength δ being equal to 1.0Ω, 4.0Ω, and 7.0Ω, respectively; the dash or dot lines corresponding to the 1-st–3-rd zeroes of the $J_0(\delta/\Omega)$.

5. Summary

We have conducted a theoretical investigation into the TS evolution of a qubit coupled to a zero-temperature reservoir, focusing on the influence of frequency modulation. Our detailed analysis revealed that carefully chosen modulation parameters, such as δ and Ω, can greatly enhance the qubit's TS in weak and strong coupling regimes. By quantitatively evaluating the power of the TS, we have demonstrated the signif-

icant improvements achieved through frequency modulation. These findings offer valuable insights for modifying and enhancing the TS in the presence of decoherence. Additionally, our numerical results have indicated that the best preservation of TS can be achieved by adjusting the ratio δ/Ω according to the zeroes of the 0-th Bessel function $J_0(\delta/\Omega)$. These optimal modulation parameters have proven instrumental in enabling the qubit's TS to persist for extended periods, even in the face of detrimental environmental noise. By analyzing the non-Markovianity, we show that the long-time preservation of TS is directly linked to the memory effect in the strong coupling regime.

Acknowledgment

Project supported by the National Natural Science Foundation of China (Grant No. 62375140).

References

[1] Wiseman H M, Jones S J and Doherty A C 2007 *Phys. Rev. Lett.* **98** 140402
[2] Jones S J, Wiseman H M and Doherty A C 2007 *Phys. Rev. A* **76** 052116
[3] Skrzypczyk P, Navascués M and Cavalcanti D 2014 *Phys. Rev. Lett.* **112** 180404
[4] Cavalcanti D and Skrzypczyk P 2017 *Rep. Prog. Phys.* **80** 024001
[5] Piani M and Watrous J 2015 *Phys. Rev. Lett.* **114** 060404
[6] Sainz A B, Aolita L, Brunner N, Gallego R and Skrzypczyk P 2016 *Phys. Rev. A* **94** 012308
[7] Händchen V, Eberle T, Steinlechner S, Samblowski A, Franz T, Werner R F and Schnabel R 2012 *Nat. Photon.* **6** 596
[8] Bowles J, Vértesi T, Quintino M T and Brunner N 2014 *Phys. Rev. Lett.* **112** 200402
[9] Zhu D, Shang W M, Zhang F L and Chen J L 2022 *Chin. Phys. Lett.* **39** 070302
[10] Chen Y Y, Guo F Z, Wei S H and Wen Q Y 2023 *Chin. Phys. B* **32** 040309
[11] Yang H, Xing L L, Ding Z Y, Zhang G and Ye L 2022 *Chin. Phys. B* **31** 090302
[12] Wollmann S, Walk N, Bennet A J, Wiseman H M and Pryde G J 2016 *Phys. Rev. Lett.* **116** 160403
[13] Branciard C, Cavalcanti E G, Walborn S P, Scarani V and Wiseman H M 2012 *Phys. Rev. A* **85** 010301
[14] He Q Y, Rosales-Zárate L, Adesso G and Reid M D 2015 *Phys. Rev. Lett.* **115** 180502
[15] Cheng W W, Wang B W, Gong L Y and Zhao S M 2021 *Quantum Inf. Processing* **20** 371
[16] Li C M, Chen K, Chen Y N, Zhang Q, Chen Y A and Pan J W 2015 *Phys. Rev. Lett.* **115** 010402
[17] Wang Y, Hao Z Y, Li J K, Liu Z H, Sun K, Xu J X, Li C F and Guo G C 2023 *Phys. Rev. Lett.* **130** 200202
[18] Cavalcanti E G, Jones S J, Wiseman H M and Reid M D 2009 *Phys. Rev. A* **80** 032112
[19] Schneeloch J, Broadbent C J, Walborn S P, Cavalcanti E G and Howell J C 2013 *Phys. Rev. A* **87** 062103
[20] Zhen Y Z, Zheng Y L, Cao W F, Li L, Chen Z B, Liu N L and Chen K 2016 *Phys. Rev. A* **93** 012108
[21] Chen Y N, Li C M, Lambert N, Chen S L, Ota Y, Chen G Y and Nori F 2014 *Phys. Rev. A* **89** 032112
[22] Chen S L, Lambert N, Li C M, Miranowicz A, Chen Y N and Nori F 2016 *Phys. Rev. Lett.* **116** 020503
[23] Bartkiewicz K, Černoch A, Lemr K, Miranowicz A and Nori F 2016 *Phys. Rev. A* **93** 062345
[24] Ku H Y, Chen S L, Chen H B, Lambert N, Chen Y N and Nori F 2016 *Phys. Rev. A* **94** 062126
[25] Liu B, Huang Y and Sun Z 2018 *Ann. Phys.* **530** 1700373
[26] Cheng W W, Chen M, Gong L Y and Zhao S M 2021 *Eur. Phys. J. D* **75** 75
[27] Cheng W W and Li B 2023 *Quantum Inf. Processing* **22** 294
[28] Lo Franco R, DArrigo A, Falci G, Compagno G and Paladino E 2014 *Phys. Rev. B* **90** 054304
[29] Xu J S, Sun K, Li C F, Xu X Y, Guo G C, Andersson E, Lo Franco R and Compagno G 2013 *Nat. Commun.* **4** 2851
[30] Xue S B, Wu R B, Zhang W M, Zhang J, Li C W and Tarn T J 2012 *Phys. Rev. A* **86** 052304
[31] Man Z X, Xia Y J and An N B 2012 *Phys. Rev. A* **86** 052322
[32] Man Z X, Xia Y J and Lo Franco R 2015 *Phys. Rev. A* **92** 012315
[33] Maniscalco S, Francica F, Zaffino R L, Gullo N L and Plastina F 2008 *Phys. Rev. Lett.* **100** 090503
[34] Campos Venuti L, Ma Z, Saleur H and Haas S 2017 *Phys. Rev. A* **96** 053858
[35] Silveri M P, Tuorila J A, Thuneberg E V and Paraoanu G S 2017 *Rep. Prog. Phys.* **80** 056002
[36] Huang J F, Liao J Q, Tian L and Kuang L M 2017 *Phys. Rev. A* **96** 043849
[37] Beaudoin F, da Silva M P, Dutton Z and Blais A 2012 *Phys. Rev. A* **86** 022305
[38] Han X, Wang D Y, Bai C H, Cui W X, Zhang S and Wang H F 2019 *Phys. Rev. A* **100** 033812
[39] Ficek Z, Seke J, Soldatov A V and Adam G 2001 *Phys. Rev. A* **64** 013813
[40] Yan Y Y, Lü Z G, Luo J Y and Zheng H 2018 *Phys. Rev. A* **94** 033817
[41] Janowicz M 2000 *Phys. Rev. A* **61** 025802
[42] Zhou L, Yang S, Liu Y X, Sun C P and Nori F 2009 *Phys. Rev. A* **80** 062109
[43] Deng C, Orgiazzi J L, Shen F, Ashhab S and Lupascu A 2015 *Phys. Rev. Lett.* **115** 133601
[44] Macovei M and Keitel C H 2014 *Phys. Rev. A* **90** 043838
[45] Agarwal G S 1999 *Phys. Rev. A* **61** 013809
[46] Mortezapour A and Lo Franco R 2018 *Sci. Rep.* **8** 14304
[47] Nourmandipour A and Mortezapour A 2023 *Quantum Inf. Processing* **22** 254
[48] Forozesh M, Mortezapour A and Nourmandipour A 2021 *Eur. Phys. J. Plus* **136** 778
[49] Rajabalinia A, Shadfar M K, Nosrati F, Mortezapour A, Morandotti R and Lo Franco R 2022 *Phys. Rev. A* **106** 062431
[50] Poggi P M, Lombardo F C and Wisniacki D A 2017 *Europhys. Lett.* **118** 20005
[51] Bellomo B, Lo Franco R and Compagno G 2007 *Phys. Rev. Lett.* **99** 160502
[52] Breuer H P, Laine E M and Piilo J 2009 *Phys. Rev. Lett.* **103** 210401
[53] Xu Z Y, Luo S, Yang W L, Liu C and Zhu S Q 2014 *Phys. Rev. A* **89** 012307